

Taking Shortcuts for Categorical VQA Using Super Neurons

Pierre Musacchio¹, Jaeyi Jeong², Dahun Kim³, and Jaesik Park¹

¹ Seoul National University

² EPFL

³ Google Deepmind

{pmusacchio, jaesik.park}@snu.ac.kr

Abstract. Sparse Attention Vectors (SAVs) have emerged as an excellent training-free alternative to supervised finetuning or low-rank adaptation to improve the performance of vision-language models (VLMs). At their heart, SAVs select a few accurate attention heads for a task of interest and use them as classifiers, rather than relying on the model’s prediction. In a similar spirit, we find that directly probing the raw activations of the VLM, in the form of scalar values, is sufficient to yield accurate classifiers on diverse visually grounded downstream tasks. Shifting focus from attention vectors to scalar activations dramatically increases the search space for accurate parameters, allowing us to find more discriminative neurons immediately from the first generated token. We call such activations Super Neurons (SNs). In this probing setting, we discover that enough SNs appear in the shallower layers of the large language model to allow for extreme early exiting from the first layer of the model at the first generated token. Compared to the original network, SNs robustly improve the classification performance while achieving a speedup of up to $5.10\times$.

1 Introduction

Vision-language model (VLM) are frontier models extending the generative capabilities of large language model (LLM) via visual grounding [1, 6, 23, 25]. Usually consisting of billions of parameters, these models retain extensive knowledge from internet-scale pretraining [4, 8, 30, 33, 39]. Although remarkably effective, their complexity hinders attempts to understand how they operate at their core.

Current research on VLM explainability and efficiency improvement mainly focuses on what could be called *macro*-level representations. That is, multi-dimensional representations that are learned through aggregating information from interactions of the tokens in the model. The most famous examples lie in linear probing [35, 42] or attention map extraction [17, 27]. However, thanks to the over-parameterization of current state of the art networks, we hypothesize that models accumulate such a tremendous amount of information over training that their individual activation scalars are sufficient to provide accurate answers to specific questions. We term these *micro*-level representations.

Thus, we repurpose the neuron activations of the model into predictions via a simple training-free strategy inspired by [27]. Analogously, we gather a probing dataset and perform an end-to-end VLM inference on it. During the process, we store activations from the large language model (LLM) of the VLM. However, instead of clustering attention heads, we directly convert the raw activations into classification predictions by thresholding them. We observe that this simple conversion scheme is enough for a subset of neurons to achieve high scores on conventional categorical visual question answer metrics for a wide diversity of datasets. We subsequently deem them *Super Neurons* (SNs). Surprisingly, SNs obtain even better performance than the models themselves on a diverse suite of unseen categorical VQA validation benchmarks. Since there are more raw activations than attention heads in the network (cf. Fig. 2b), there are more chances to find SNs that have desirable properties, such as better performance and robustness. Specifically, we discover that some SNs located in shallower layers of the model preserve great performance even while the first token is being generated. This allows us to perform *extreme early exit* *i.e.* interrupt inference on the first layer of the LLM during the generation of the first token.

Our contributions are summarized as follows:

- We shift the analysis from *macro*-level representations (akin to attention vectors) to *micro*-level ones (scalar activations). By doing so, we present a training-free approach that identifies high-scoring neurons in the LLM of the VLMs,
- We comprehensively benchmark the probed neurons and find that they can serve as strong categorical classifiers, *outperforming the base models themselves* on a diverse suite of VQA benchmarks. We therefore call them *Super Neurons*,
- We thoroughly investigate SNs (discriminative power, location in the model, quantity, robustness) and introduce the *agreement rate* metric that quantifies the divergence between SNs predictions and model predictions,
- As a byproduct, SNs enable extreme early exit at inference time, providing a speedup of up to 5.10× while maintaining model-level performance.

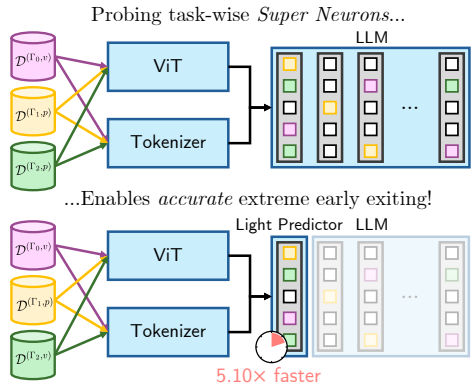


Fig. 1: Overview of our approach. Our training-free scheme uncovers Super Neurons (SNs) via probing data. They robustly outperform the base model on a variety of categorical VQA datasets. As a byproduct, they enable *extreme early exiting* at the first layer of the LLM on the first generated token. Colored boxes in the LLM represent SNs for their data types.

2 Related work

Efficient VLMs. A conventional approach to turn large VLMs to efficient models is to prune them at the parameter level, either by distillation [40] or by training a policy to search which weights to remove [22]. Pruning can also occur at the token level, usually via token similarity approaches [5, 14, 41, 43], by estimating visual contribution [24], or using scale-down approaches [25]. If the final objective is to improve performance, training a robust visual encoder is also a viable solution [9, 37]. Some approaches diverge by considering early exit from the model, either in a supervised setting [2] or in a training-free manner by estimating layer-wise similarities [36]. Recently, task vectors [11] have been leveraged in VLMs in the form of sparse attention vectors to enable training-free improvement of VLMs in classification tasks [27]. Single modality convnets and LSTMs can rely on some of their weights for accurate prediction [19, 32], but this remains to be shown for transformers, specifically when processing multimodal tokens.

While inspired by [27], we elect neural activations rather than clustering attention heads, shifting the representation of interest from a macro- to a micro-level (cf. Fig. 2a). This shift continues to hold properties reported in [19, 27, 32] (e.g. better performance than the model itself), while being robust to prompt variations and distribution shifts, enabling inference on diverse VQA tasks and extreme early stopping.

Although we solely focus on categorical VQA tasks, we propose a training-free approach that identifies expert neural activations and establishes a set of SNs that solves the task accurately and robustly, without relying on token similarity or altering model weights. After discovery, we substantially improve the runtime performance of VLM using extreme early exit, as early as the first layer.

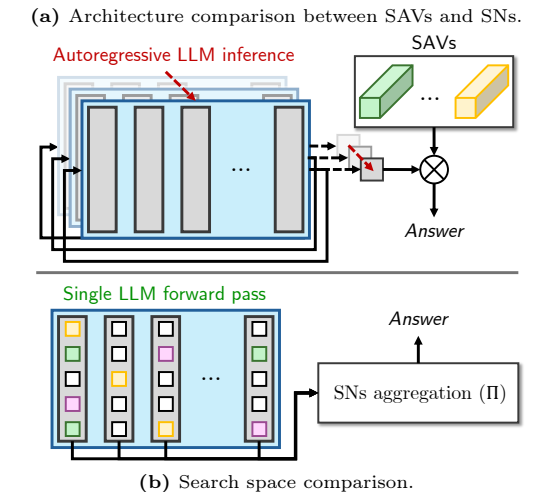


Fig. 2: Comparison between SAVs and ours. We show architectural divergences in Fig. 2a and resulting search spaces of the two approaches for LLaVA-v1.5-7b in Fig. 2b.

Explainable VLMs. Model explainability is a fundamental challenge for the deployment of VLMs in the real world. Since VLMs are increasingly being

Algorithm 1: SUPER NEURONS EXTRACTION

Data: $\mathcal{D}^{(\Gamma,p)}$, probing dataset for task Γ ; E_{vis} and E_{txt} , vision and text encoders of the VLM; f , LLM of the VLM; α , activation threshold parameter; μ , a function that computes a metric; \mathbf{Y} , ground-truths;SN t , super neurons threshold.

```

1  $\mathbf{H}^{(\Gamma,p)} \leftarrow \{\}$ 
2 for  $\mathbf{I}_n^{(\Gamma,p)}, \mathbf{T}_n^{(\Gamma,p)} \in \mathcal{D}^{(\Gamma,p)}$  do
3    $\mathbf{H}_n^{(\Gamma,p)} \leftarrow f(E_{\text{vis}}(\mathbf{I}_n^{(\Gamma,p)}); E_{\text{txt}}(\mathbf{T}_n^{(\Gamma,p)}))$ ;
4    $\mathbf{H}^{(\Gamma,p)}. \text{APPEND}(\mathbf{H}_n^{(\Gamma,p)})$ ;
5  $\mathbf{H}^{(\Gamma,p)} \leftarrow \mathbf{H}^{(\Gamma,p)} > \alpha$ ;
6  $\mathbf{S}_\mu^{(\Gamma,p)} \leftarrow \mu(\mathbf{H}^{(\Gamma,p)}, \mathbf{Y})$ ;
7  $\Sigma = \text{idx } \mathbf{H}^{(\Gamma,p)}[\mathbf{S}_\mu^{(\Gamma,p)} > \text{SN}t]$ ;
8 return  $\Sigma$ ;

```

adopted as master operators in robotics [3, 18, 44], guardrails must be set up to ensure the security of their behavior. Substantial work has led to a better understanding of how attention, which VLMs are usually built on, behaves. Notably, CLIP-Dissects proposes tagging each neuron in the transformer with a concept [29], showing that transformers learn more complex patterns as the representation is forwarded down its layers. Efforts have also been directed towards understanding attention sinks [7, 16, 31]. Moreover, due to the extensive number of attention operations in the LLM of the VLM, the community has reported the emergence of object-aligned attention maps in the transformer decoder of the architecture [17]. Linear probing approaches tend to show that the VLM generates its answer based on different stages of reasoning [42], yet, these stages do not seem to be monolithic [27, 35]. Sparse autoencoders has shown that some specific neurons hold object-specific concepts [13, 38].

In our work, we propose studying the capabilities of individual neurons without adding a single learning component that could alter the understanding of their function. By repurposing raw activations as categorical predictions, we show that VLMs possess expert neurons across a diverse set of tasks. Analyzing the location of the emergence of these neurons helps us better understand that the LLM is in principal capable of answering a question sometimes as early as in the *first layer* of the LLM when generating the *first token* of the answer. We also investigate to what extent SNs and the model disagree by introducing the agreement rate (AR) metric. Robustness experiments suggest that SNs are *not* exploiting spurious correlations of the input data and generalize to new distributions or neighboring prompts, suggesting the universality of our approach.

Algorithm 2: SUPER NEURONS INFERENCE

Data: E_{vis} and E_{txt} , vision and text encoders of the VLM; f , LLM of the VLM; α , activation threshold parameter;

SNt, super neurons threshold;

 Σ , indexing of previously probed SNs; Π , an aggregation function.

- 1 $\mathbf{H}^{(T,v)} \leftarrow \{\}$
 - 2 **for** $\mathbf{I}_n^{(T,v)}, \mathbf{T}_n^{(T,v)} \in \mathcal{D}^{(T,v)}$ **do**
 - 3 $\mathbf{H}_n^{(T,v)} \leftarrow f(E_{\text{vis}}(\mathbf{I}_n^{(T,v)}); E_{\text{txt}}(\mathbf{T}_n^{(T,v)}))$;
 - 4 $\mathbf{H}^{(T,v)}.APPEND(\mathbf{H}_n^{(T,v)})$;
 - 5 $\mathbf{H}^{(T,v)} \leftarrow \mathbf{H}^{(T,v)} > \alpha$;
 - 6 **return** $\Pi(\mathbf{H}^{(T,v)}[\Sigma])$;
-

3 Method

3.1 Preliminaries

Notations. We define a VLM as the combination of vision and text encoders $E_{\text{vis}} : \mathbb{R}^{H \times W \times 3} \rightarrow \mathbb{R}^{s_{\text{vis}} \times D}$ and $E_{\text{txt}} : \mathbb{N}^s \rightarrow \mathbb{R}^{s_{\text{txt}} \times D}$ that feed their output to an LLM $f : \mathbb{R}^{(s_{\text{vis}} + s_{\text{txt}} + 1) \times D} \rightarrow \mathbb{R}^{(s_{\text{vis}} + s_{\text{txt}} + 1) \times D}$. Given a grounding image $\mathbf{I} \in \mathbb{R}^{H \times W \times 3}$ and a text prompt $\mathbf{T} \in \mathbb{N}^s$, a VLM forward pass is defined as follows:

$$\hat{\mathbf{Y}}^{s+1} = f(E_{\text{vis}}(\mathbf{I}); E_{\text{txt}}(\mathbf{T})). \quad (1)$$

Here, $\hat{\mathbf{Y}}^{s+1}$ can be auto-regressively fed into f . This process ends when the LLM generates an `<eos>` token. Moreover, given an $L \in \mathbb{N}$ layered LLM, we denote $\mathbf{H}_l \in \mathbb{R}^D$ the activation extracted from the l -th layer. For clarity, we omit the subscript when referring to the full set of L activations, *i.e.* $\mathbf{H} \in \mathbb{R}^{L \times D}$.

Problem. Conventional VLMs are built from an LLM architecture that contains billions of parameters, processing both vision and text tokens. We hypothesize that this parametric scale is reasonable for individual neurons to hold critical information about the answer for a given text-image pair and that we do not necessarily need the full model to answer the question. Specifically, we claim that *some scalar activations are sufficient to provide a satisfactory answer, on par or even better than the full model itself*. We call these hypothetical neuron outputs *Super Neurons* (SNs). Inspired by [27], our work provides a simple setup to discover such SNs for categorical VQA.

Uncovering SNs can be thought of as a three-step process. First, we gather a *probing set*. We then perform a forward pass of the network on the probing set to uncover neurons that have high activations on it based on a metric to optimize. Finally, we evaluate SNs on the validation set of the dataset to assess their performance. We provide the complete algorithm used to discover SNs in Algorithm 1.

3.2 Super Neurons

Probing set. Formally, we identify a task Γ to solve and gather a probing dataset $\mathcal{D}^{(\Gamma,p)} = \left\{ \mathcal{D}_n^{(\Gamma,p)} \right\}_{n=0}^{N \in \mathbb{N}}$. Here, p stands for *probing set*. This probing set is typically built from training data used to optimize a model for Γ . We gather the full model activations for each of the vision-text pairs of the probing set $(\mathbf{I}_n^{(\Gamma,p)}, \mathbf{T}_n^{(\Gamma,p)}) \in \mathcal{D}_n^{(\Gamma,p)}$:

$$\mathbf{H}_n^{(\Gamma,p)} = f(E_{\text{vis}}(\mathbf{I}_n^{(\Gamma,p)}); E_{\text{txt}}(\mathbf{T}_n^{(\Gamma,p)})) \in \mathbb{R}^{L \times D}. \quad (2)$$

Taking into account all samples in the dataset, we note $\mathbf{H}^{(\Gamma,p)} \in \mathbb{R}^{N \times L \times D}$ the tensor of all activations.

Discovering Super Neurons. The key idea is to directly convert the raw activations into binary predictions. Hence, we introduce a threshold variable $\alpha \in \mathbb{R}$ responsible for binarizing the raw activations:

$$\mathbf{H}^{(\Gamma,p)} > \alpha. \quad (3)$$

We detail how we instantiate this value in Sec. 4.2.

We proceed to evaluate each neuron on the full probing set using a predetermined metric μ to acquire neuron-level statistics:

$$\mathbf{S}_\mu^{(\Gamma,p)} = \mu \left(\mathbf{H}_n^{(\Gamma,p)}, \mathbf{Y}_n \right), \quad \forall n \in \{0, \dots, N\}, \quad (4)$$

where \mathbf{Y}_n is the ground-truth for the n -th data sample and $\mathbf{S}_\mu^{(\Gamma,p)} \in [0, 1]^{N \times L}$ represents the neuron-wise scores for task Γ on the probing set p with respect to a metric μ . Conventional metrics are usually normalized from 0 to 1. Therefore, we consider this formulation.

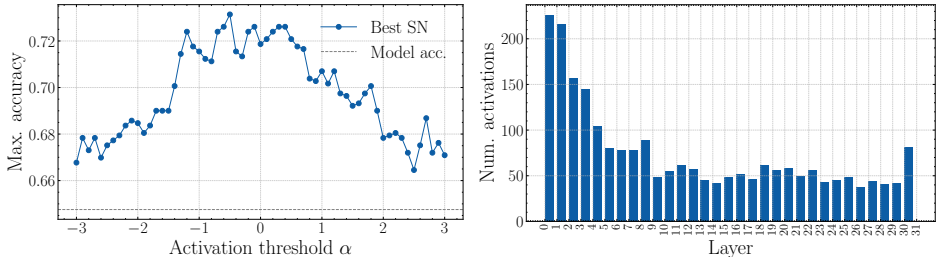
At this stage, we identify neurons as super neurons if they fall above a specific predetermined metric threshold. We call this threshold $\text{SN}t \in [0, 1]$. Thus, the final SNs are selected as follows:

$$\Sigma = \text{idx } \mathbf{H}^{(\Gamma,p)} [\mathbf{S}_\mu^{(\Gamma,p)} > \text{SN}t]. \quad (5)$$

Hence, Σ represents the index map of the thresholded SNs for a given $\text{SN}t$ and idx is a function that returns the indices of the tensor values that meet the thresholding requirement.

Evaluating Super Neurons on validation data. Once Σ is obtained, we perform the inference on the validation set of Γ denoted $\mathcal{D}^{(\Gamma,v)} = \left\{ \mathcal{D}_n^{(\Gamma,v)} \right\}_{n=0}^N$, where v stands for *validation set*. As with the probing set, we extract $\mathbf{H}^{(\Gamma,v)}$ and only select SN activations from indexing on Σ :

$$\hat{\mathbf{Y}}^* = \mathbf{H}^{(\Gamma,v)}[\Sigma] > \alpha, \quad (6)$$

(a) Accuracy w.r.t. the activation threshold α .

(b) Number of SNs per layer.

Fig. 3: Empirical analysis of SNs. Figure 3a shows the maximum accuracy on the probing set with respect to different α . We evaluate α over the range $\alpha \in [-3, 3]$. The maximum accuracy peaks around $\alpha = 0$. Figure 3b records the number of found SNs that obtain a better accuracy than the model in each layer. We use LLaVA-v1.5-7b on VizWiz for both figures.

where $\hat{\mathbf{Y}}^* \in \{0, 1\}^K$ and $K \in \mathbb{N}$ denotes the number of selected SNs. Since K is usually larger than 1, we finally aggregate all the SN predictions into a single final prediction using an aggregation function Π . For this, we use two different strategies. Either, we simply average all SN predictions or we perform majority voting. We provide the inference routine in Algorithm 2.

3.3 Agreement rate

To measure how much SNs diverge from the predictions of the model, we introduce the agreement rate (AR) metric. Conceptually, AR aims at quantifying the frequency at which SNs and the model have the same answers. We define AR as follows:

$$\text{AR} = \frac{1}{NK} \sum_{n=0}^N \sum_{k=0}^K \mathbb{1} \left(\hat{\mathbf{Y}}_{n,k}^* = \hat{\mathbf{Y}}_n \right) \in [0, 1]. \quad (7)$$

Here, $\mathbb{1}$ is the indicator function and we subscript the SNs index by k , while subscripting the data samples by n . Note that AR can be obtained for different SNt thresholds. Thus, we also denote the metric with a suffix specifying the SNt *e.g.* if SNt = 0.8, then AR@0.8 is the agreement rate across all SNs whose accuracy exceeds 0.8 on the set of interest.

4 Experiments

4.1 Datasets

We validate our approach on seven diverse categorical VQA datasets:

- POPE, for object hallucination [21],
- INSTAORDER (OCC.), for occlusion understanding [20, 28],
- INSTAORDER (DEPTH), for depth understanding,
- VIZWIZ, for broad visual understanding [10],

Table 1: Best probed SN on diverse categorical VQA datasets. We report accuracy and F1. We display the results obtained by the single best performing SN in the model. Best results are in **bold**. Baselines are highlighted in **gray**. We use a probing set size of 3,000 samples except for VIZWIZ, which only contains 942 binary questions. Accuracy and F1 are optimized separately. SNs outperform the base models in all cases.

Metric	Method	Dataset						
		POPE	INSTAORDER (DEPTH)	INSTAORDER (OCC.)	VIZWIZ	CLEVR	A-OKVQA	SCIENCEQA
Accuracy	<i>LLaVA-v1.5-7b</i>	90.7	61.7	53.9	64.8	52.3	67.8	62.2
	SN	92.5 (+1.8)	63.5 (+1.8)	62.7 (+8.8)	71.9 (+7.1)	54.4 (+2.1)	68.0 (+0.2)	63.8 (+1.6)
	<i>Qwen3-VL-4b-Instruct</i>	95.0	61.8	50.8	78.3	84.7	82.7	81.3
	SN	96.1 (+1.1)	62.8 (+1.0)	62.6 (+11.8)	81.0 (+2.7)	88.6 (+3.9)	83.0 (+0.3)	82.3 (+1.0)
F1	<i>LLaVA-v1.5-7b</i>	91.1	67.7	46.1	72.0	61.7	74.5	70.0
	SN	92.3 (+1.2)	69.1 (+1.4)	69.0 (+22.9)	74.8 (+2.8)	66.9 (+5.2)	73.8(-0.7)	70.7 (+0.7)
	<i>Qwen3-VL-4b-Instruct</i>	94.8	63.1	4.2	78.9	86.4	82.3	81.4
	SN	95.9 (+1.1)	69.1 (+6.0)	69.1 (+64.9)	81.2 (+2.3)	89.0 (+2.6)	82.6 (+0.3)	82.2 (+0.8)

- CLEVR, a synthetic dataset for geometrical understanding [15],
- A-OKVQA, a general knowledge multiple choice question (MCQ) dataset [34],
- SCIENCEQA, an MCQ dataset for mathematics and scientific reasoning [26].

We provide details of each dataset, along with their respective prompt templates, in Appendix A.

4.2 Evaluation protocol

Probing set. We construct a probing set of size $N = 3,000$ for all datasets, randomly sampled from their respective training sets. By probing samples from the training set, we ensure there is *no overlap* between the probing and validation data. We make a single exception for VIZWIZ, which contains fewer than 1K categorical VQA in its train set. We convert A-OKVQA and SCIENCEQA as a series of binary questions allowing our method to be applied indistinguishably as for other datasets. We balance the probing set of each dataset to ensure that each categorical class is evenly represented to avoid biasing the selected SNs.

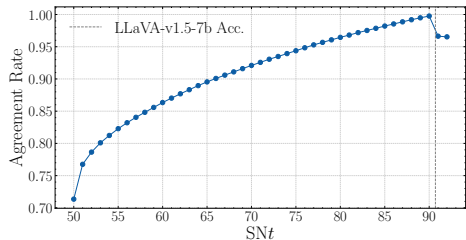


Fig. 4: Agreement rate with respect to different SNt. We compute AR on POPE using LLaVA-v1.5-7b. At lower accuracy, SNs largely agree with the model prediction. However, for SNs to obtain better results than the model, they have to disagree on some answers.

Models. We evaluate two well-established models in the VLM landscape to emphasize the universal plug-and-play nature of our approach. We choose LLaVA-v1.5-7b since it is a cornerstone VLM and has been widely adopted and mod-

Table 2: Evaluation of probed SNs on diverse categorical VQA validation datasets. We report both the mean of SNs and the majority voting with respect to the SN t found from the probing data. All SNs were optimized for accuracy on the probing set. For a given metric, best results are in **bold** and second best are underlined. Baselines are highlighted in **gray**.

Metric	Method	Dataset						
		POPE	INSTAORDER (DEPTH)	INSTAORDER (OCC.)	VIZWIZ	CLEVR	A-OKVQA	SCIENCEQA
SN t	SNs <i>LLaVA-v1.5-7b</i>	92%	63%	62%	71%	53%	67%	63%
	SNs <i>Qwen3-VL-4b-Instruct</i>	95.8%	62.6%	62.0%	80.9%	88.3%	80.0%	82.0%
Accuracy	<i>LLaVA-v1.5-7b</i>	89.8	65.0	<u>64.9</u>	65.6	51.3	54.8	<u>53.5</u>
	SNs (mean)	90.9 ^(+1.1)	66.1 ^(+1.1)	64.5 ^(-0.4)	72.6 ^(+7.0)	51.5 ^(+0.2)	<u>61.4</u> ^(+6.6)	57.4 ^(+6.9)
	SNs (maj. voting)	90.9 ^(+1.1)	65.2 ^(+0.2)	78.2 ^(+13.3)	<u>69.9</u> ^(+4.3)	<u>51.4</u> ^(+0.1)	72.0 ^(+17.2)	48.4 ^(-5.1)
	<i>Qwen3-VL-4b-Instruct</i>	91.5	63.4	85.2	81.7	83.7	85.2	81.1
	SNs (mean)	<u>93.4</u> ^(+1.9)	<u>63.6</u> ^(+0.2)	78.1 ^(-7.1)	<u>81.2</u> ^(-0.5)	88.3 ^(+4.6)	85.2 ^(+0.0)	82.9 ^(+1.8)
	SNs (maj. voting)	93.7 ^(+2.2)	64.9 ^(+1.5)	77.2 ^(-8.0)	80.1 ^(-1.6)	88.3 ^(+4.6)	85.2 ^(+0.0)	<u>82.4</u> ^(+1.3)
Precision	<i>LLaVA-v1.5-7b</i>	89.5	66.4	18.5	60.1	<u>50.9</u>	34.9	<u>40.1</u>
	SNs (mean)	92.6 ^(+3.1)	68.8 ^(+2.4)	23.5 ^(+5.0)	73.9 ^(+13.9)	51.0 ^(+1.0)	<u>37.7</u> ^(+2.8)	42.4 ^(+2.3)
	SNs (maj. voting)	<u>91.0</u> ^(+0.5)	<u>66.4</u> ^(+0.0)	30.4 ^(+11.9)	<u>64.1</u> ^(+4.0)	<u>50.9</u> ^(+0.0)	44.7 ^(+9.8)	38.3 ^(-1.7)
	<i>Qwen3-VL-4b-Instruct</i>	98.5	69.3	49.6	80.4	76.7	66.0	68.3
	SNs (mean)	<u>97.6</u> ^(-0.9)	70.1 ^(+0.8)	31.3 ^(-18.3)	76.9 ^(-3.5)	87.9 ^(+11.2)	66.0 ^(+0.0)	<u>71.7</u> ^(+3.4)
	SNs (maj. voting)	96.5 ^(-2.0)	69.2 ^(-0.1)	29.2 ^(-20.4)	<u>79.8</u> ^(-0.6)	<u>85.3</u> ^(+8.6)	66.0 ^(+0.0)	72.9 ^(+4.6)
Recall	<i>LLaVA-v1.5-7b</i>	90.8	80.2	40.2	92.5	76.6	93.9	85.9
	SNs (mean)	89.5 ^(-1.3)	75.9 ^(-5.3)	61.8 ^(+21.6)	69.9 ^(-22.6)	75.8 ^(-0.8)	83.7 ^(-10.2)	84.5 ^(-1.4)
	SNs (maj. voting)	91.4 ^(+0.6)	80.9 ^(+0.7)	36.5 ^(-3.7)	<u>90.3</u> ^(-2.2)	77.5 ^(+0.9)	51.8 ^(-42.1)	94.9 ^(+9.0)
	<i>Qwen3-VL-4b-Instruct</i>	84.9	<u>66.0</u>	2.7	<u>83.9</u>	96.8	83.8	78.7
	SNs (mean)	<u>89.3</u> ^(+4.4)	64.8 ^(-1.2)	40.0 ^(+37.3)	89.2 ^(+5.3)	90.0 ^(-6.8)	83.7 ^(-0.1)	78.3 ^(-0.4)
	SNs (maj. voting)	91.1 ^(+6.2)	71.1 ^(+5.1)	<u>37.8</u> ^(+35.1)	80.6 ^(-3.3)	<u>92.5</u> ^(+4.3)	83.8 ^(+0.0)	<u>73.4</u> ^(+5.3)
F1	<i>LLaVA-v1.5-7b</i>	90.2	<u>72.6</u>	25.3	<u>72.9</u>	<u>61.1</u>	<u>50.9</u>	<u>54.7</u>
	SNs (mean)	<u>91.0</u> ^(+0.8)	72.2 ^(-0.4)	34.0 ^(+8.7)	71.8 ^(-1.1)	61.0 ^(-0.1)	52.0 ^(+0.1)	56.5 ^(+1.8)
	SNs (maj. voting)	91.2 ^(+1.0)	72.9 ^(+0.3)	<u>33.2</u> ^(+7.9)	75.0 ^(+2.1)	61.4 ^(+0.3)	48.0 ^(-2.9)	54.6 ^(-0.1)
	<i>Qwen3-VL-4b-Instruct</i>	91.2	<u>67.6</u>	5.1	<u>82.1</u>	85.6	<u>73.8</u>	73.1
	SNs (mean)	<u>93.3</u> ^(+2.1)	67.4 ^(-0.2)	35.1 ⁽⁺³⁰⁾	82.6 ^(+0.5)	89.0 ^(+3.4)	<u>73.8</u> ^(+0.0)	74.8 ^(+1.7)
	SNs (maj. voting)	93.7 ^(+2.5)	70.1 ^(+2.5)	<u>33.0</u> ^(+27.9)	80.2 ^(-1.9)	<u>88.7</u> ^(+3.1)	73.9 ^(+0.1)	<u>73.2</u> ^(+0.1)

ified [23, 25]. We also experiment on the more recently released Qwen3-VL-4b-Instruct as its capabilities are known to be better than LLaVA-v1.5-7b while being significantly smaller [1]. Finally, we conduct scaling-up experiments using LLaVA-v1.5-13b and Qwen3-VL-32b-Instruct. Unless specified otherwise, we use the default model configuration in all cases. Further information can be found in appendix B.

Experimental setting. Unless mentioned otherwise, we use NVIDIA RTX A6000 GPUs for our experiments. The extraction of SNs is training-free and simply requires the collection of raw activations from the model. Split across 8 GPUs, this only requires about 4 minutes of runtime for LLaVA-v1.5-7b. To find the optimal α activation threshold, we first compute the mean activation across 3K randomly sampled VQA in the POPE-style format, yielding 0.0083. We also empirically pick different α values in the probing set

Table 3: Comparison of SNs and SAVs. We benchmark LLaVA-v1.5-7b on VIZWIZ using the same number of probing samples N . Best performing method is in **yellow**.

Method	N	Acc.	Prec.	Recall	F1
SAVs [27]	40	51.8	50.6	95.7	66.1
SNs (ours)	40	60.2	56.8	84.9	68.1

of VIZWIZ in Fig. 3a. Interestingly,

Table 4: Performances of SNs for scaled-up models. After probing SNs following our method, we report the validation results of LLaVA-v1.5-13b and Qwen3-VL-32b-Instruct on POPE and SCIENCEQA respectively. Best performances for a given optimized metric are in bold, baseline performance is in gray .

(a) LLaVA-v1.5-13b on POPE.					(b) Qwen3-VL-32b-Instruct on SCIENCEQA.						
Opt. Metric	Method	POPE				Opt. Metric	Method	SCIENCEQA			
		Acc.	Prec.	Recall	F1			Acc.	Prec.	Recall	F1
	<i>Vanilla model</i>	88.7	85.6	94.0	89.6		<i>Vanilla model</i>	81.4	67.5	82.9	74.4
Accuracy	SNs (mean)	88.8	85.7	94.1	89.7	Accuracy	SNs (mean)	84.9	75.5	79.4	77.4
	SNs (maj. voting)	87.6	83.4	94.9	88.8		SNs (maj. voting)	84.8	76.6	77.4	77.0
F1	SNs (mean)	88.9	85.5	94.4	89.7	F1	SNs (mean)	84.0	73.6	79.5	76.5
	SNs (maj. voting)	85.9	85.7	87.2	86.4		SNs (maj. voting)	85.0	76.3	78.2	77.2

all tested values provide accuracy above the model itself. Nevertheless, this figure confirms that the maximum accuracy peaks around $\alpha = 0$. Thus, we use $\alpha = 0$ for all experiments. After running Algorithm 1 on the probing set of each dataset, we choose the appropriate SN_t by sweeping across values that are up to 3 points lower using a step size of 1 for LLaVA-v1.5-7b and a step of 0.1 for Qwen3-VL-4b-Instruct. We use 128 max. generated tokens, set temperature to 0, use 1 beam, and don't leverage stop strings in all experiments, unless stated otherwise. We detail the configurations of the models in appendix B.

Metrics. To account for the fact that VQA benchmarks can be imbalanced, not only do we report accuracy, as previous works do, but also compute precision, recall, and F1 score. This allows us to better estimate the predictive capabilities of all benchmarked methods. We use a rule-based evaluation strategy for accurate and interpretable results. Accuracy, precision, recall and F1 are defined as follows:

$$\text{Accuracy} = \frac{1}{N} \sum_n \mathbb{1}(\hat{\mathbf{Y}}_n^* = \mathbf{Y}_n), \quad (8)$$

$$\text{Precision} = \frac{\sum_n \mathbb{1}(\hat{\mathbf{Y}}_n^* = 1 \wedge \mathbf{Y}_n = 1)}{\sum_n \mathbb{1}(\hat{\mathbf{Y}}_n^* = 1)}, \quad (9)$$

$$\text{Recall} = \frac{\sum_n \mathbb{1}(\hat{\mathbf{Y}}_n^* = 1 \wedge \mathbf{Y}_n = 1)}{\sum_n \mathbb{1}(\mathbf{Y}_n = 1)}, \quad (10)$$

$$\text{F1} = \frac{2 \times \text{Precision} \times \text{Recall}}{\text{Precision} + \text{Recall}}. \quad (11)$$

Following the previously established notations, N denotes the size of the dataset, n a sample index, $\hat{\mathbf{Y}}^*$ a prediction made from an SN and \mathbf{Y} the ground-truth label. At probing time, these metrics can serve as a choice of μ . We also

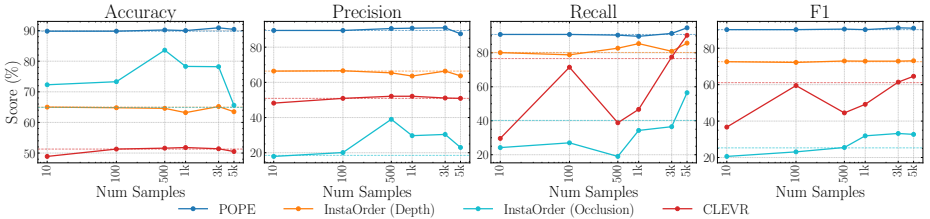


Fig. 5: Super Neurons performances with respect to different probing set sizes. We compute accuracy, precision, recall and F1 on diverse benchmarks using LLaVA-v1.5-7b. Dashed lines (colors matching their respective datasets) indicate the performance of the vanilla model. Overall, more data leads to performance improvements.

compute them on the model output. During validation, we recompute these metrics on the model and the elected SNs to obtain the numbers reported in the benchmarks.

4.3 Results

SNs extraction. We start by gathering SNs from the probing set. We report the performance of the *single best* scoring neuron in Tab. 1. In this table, we optimize for two main metrics $\mu = \{\text{accuracy, F1}\}$ and report their respective results in different rows. We observe that the highest-scoring neuron surpasses the model on all probed datasets. We specifically note large differences on VIZWIZ and INSTAORDER (OCC.), tasks that are most likely out-of-distribution relative to LLaVA and Qwen’s pre-training mix. We remark a particular weakness of Qwen when prompted on INSTAORDER (OCC.). We noted that the model consistently answered “no”, resulting in an extremely low F1. On the other hand, our SNs are able to robustly classify these examples in the probing set. We highlight tricky cases where SNs are accurate in Fig. 6. Still in this figure, the A-OKVQA case shows that the model sometimes does not have a clear representation of the concept described in the image, as it replies equally for each type of pepper. On the other hand, SNs manage to sharply determine which type of pepper is sold.

We investigate the quantity of probed neurons in Fig. 3b. Since we behave at the scalar-level and not at the vector-level anymore, we observe a large amount of accurate SNs. It is especially interesting to note that these SNs are also revealed

Table 5: Runtime benchmark on POPE. We benchmark the average runtime of LLaVA-v1.5-7b on the full validation set using *its official inference code*. L^* indicates the inference exit layer. All numbers are recorded using a single NVIDIA RTX A6000. Best performances are in **bold**. Baseline is in gray, and best runtime is in yellow.

Inference Strategy	Autoreg. L^*	Acc.	F1	Runtime (s.)
Model	LLaVA-v1.5-7b	✓	32 89.8 90.2	0.78
SNs	$SNt = 0.92$ (maj. vote)	✗	15 90.9 91.2	0.16(-4.81×)
	$SNt = 0.91$ (mean)	✗	12 90.6 90.8	0.16(-4.87×)
	$SNt = 0.90$ (maj. vote)	✗	1 89.8 90.2	0.15(-5.10×)

in the shallowest layers of the LLM, suggesting that individual neurons might be involved in the decision process of the network earlier than expected [42].

To further attempt to understand how SNs behave with respect to the predictions of the model, we plot the AR curve for different SN t in the probing test of POPE in Fig. 4. We observe a clear logarithmic trend in the agreement between LLaVA and SNs until they reach the same performance. Beyond this point, we observe a sharp AR drop, indicating that neurons must significantly disagree with the model to obtain more accurate answers. This makes sense: the base model provides a lower bound performance if the SNs only agree with it. They need to make more accurate predictions to surpass it, and therefore must disagree with it more often.

Main evaluation. We then evaluate the probed SNs in the validation set of our selected dataset suite in Tab. 2. We observe that SNs largely outperform or perform competitively against the model from which they are extracted. Superior results on both LLaVA-v1.5-7b and Qwen3-VL-4b-Instruct support the universality of our approach. Interestingly, Qwen performs extremely poorly on the occlusion understanding task, whereas our method is sufficient to raise its F1 score above that of vanilla LLaVA. Our method continues to provide strong results for challenging MCQ datasets (A-OKVQA, SCIENCEQA), consistently outperforming the base model by a significant margin (Tab. 2).

Comparison with baselines. We compare inference with SNs against n -shot prompting in Tab. 8. For both POPE and CLEVR, n -shot prompting LLaVA-v1.5-7b results in large performance degradation as previously observed in [27]. Our proposed SNs outperform or obtain on par results with all the baselines for accuracy and F1. We also compare SNs with SAVs [27] in Tab. 3. While SAVs were originally evaluated on VIZWIZ’s “answerable”-“unanswerable” questions, we observed that this data was about 77% imbalanced towards “unanswerable” and that SAVs answers were biased towards it. Thus, we benchmark both SAVs and SNs on our balanced “yes”-“no” VIZWIZ validation set, such that the accuracy value becomes more representative of the predictive capabilities of each approach. We use the number of probing samples of SAVs (*i.e.* 40) for both approaches. We observe that SAVs’ recall is effectively high but lower accuracy, indicating high answer bias. On all metrics, SNs compare positively to SAVs.

Table 6: Impact of token selection for SNs discovery on POPE. We use LLaVA-v1.5-7b. L^* is the first possible early stopping layer. Best performing method is highlighted in yellow. Early exiting after the first token improves runtime and performances.

Token Pos.	L^*	Acc.	Prec.	Recall	F1	Runtime (s.)
Last	14	90.9	92.6	89.5	91.0	0.76
First	15	90.9	91.0	91.4	91.2	0.16 (-4.75x)

Table 7: Transfer capabilities of SNs to a novel distribution. We use the POPE format.

Method	Probe	Val.	Acc.	Prec.	Recall	F1
LLaVA-v1.5-7b	–	Voc	91.8	88.1	96.7	92.2
SNs	Voc	Voc	91.9	88.1	96.8	92.3
SNs	Coco	Voc	91.6	87.2	97.6	92.1

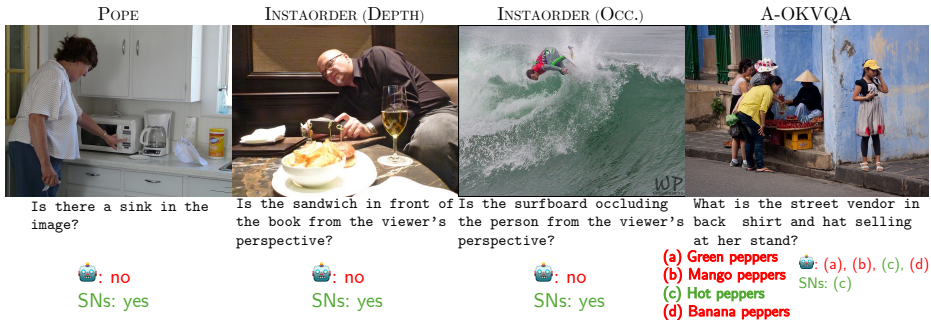


Fig. 6: Qualitative results of SNs. We show examples on diverse validation sets. We use LLaVA-v1.5-7b on POPE and INSTAORDER (OCC.) and Qwen3-VL-4b-Instruct on INSTAORDER (DEPTH) and A-OKVQA. The robot icon symbolizes the model output. Green indicate that the answer matches the ground-truth and red indicates an incorrect answer.

Runtime efficiency. We compare the full model and SNs’ inference speed in Tab. 5. By bypassing the autoregressive process, SNs dramatically reduces inference runtime while maintaining performance on par with the base model. We provide an in-depth profiling using huggingface’s inference pipeline in Tab. 4 (appendix Sec. C).

Scaling. Performance analysis confirms that SNs also emerge at larger scale for both LLaVA-v1.5-13b (Tab. 4a) and Qwen3-VL-32b-Instruct (Tab. 4b), solidifying the scalability and universality of our approach.

4.4 Ablation studies

Robustness. We evaluate the robustness of SNs with a transfer experiment in Tab. 7. We use the official POPE repository to build a POPE-VOC validation dataset. We probe on POPE built from COCO and evaluate on POPE-VOC. Although the validation distribution differs from the probing one, SNs remain competitive. We also discover that SNs are robust to prompt changes, providing evidence that they are not overfitting on probing data nor exploiting spurious biases from the inputs (cf. appendix D).

Table 8: Comparing n -shot prompting and SNs. We benchmark LLaVA-v1.5-7b. SNs are consistently more accurate.

	Num. shots	0	1	3	5	SNs
POPE	Acc.	89.8	82.3	63.0	60.8	90.9
	Prec.	89.5	84.0	84.0	81.6	91.0
	Recall	90.8	81.3	81.3	31.0	91.4
	F1	90.2	83.6	82.6	44.9	91.2
INSTAORDER (DEPTH)	Acc.	65.0	60.7	58.9	58.9	65.2
	Prec.	66.4	60.3	58.6	58.7	66.4
	Recall	80.2	93.9	98.7	97.9	80.9
	F1	72.6	73.5	73.5	73.4	72.9
CLEVR	Acc.	51.3	50.8	50.4	49.9	51.4
	Prec.	50.9	50.7	50.4	49.9	50.9
	Recall	76.6	59.2	51.2	50.7	77.5
	F1	61.1	54.6	50.8	50.3	61.4

Token selection. We consider which token provides the best performance for our approach. Contrary to SAVs [27], SNs perform better on the first token of the sequence, opening the door to *extreme early exit* by completely skipping the autoregressive process of the LLM. We further stop at the first layer of the model by lowering the SN_t while maintaining model-level performances. In that setting, inference runs 5.10× faster than the original model. We believe that this phenomenon arises from the larger search space of our approach (cf. Fig. 2b).

Data regime. Although our approach is training-free, SNs need to be gathered using probing data. To understand how this ties to final SNs performance, we sample varying probing set sizes and plot their scores over the validation set Fig. 5. Overall, the more data, the better. SNs surpass the base model performance when using more than 100 data samples. This is the same order of magnitude as the data required by SAVs [27]. Performance degrades at 5K samples, thus we default to 3K.

Metric optimization. We optimize SNs for different metrics μ in table Tab. 1. We then use the probed SNs to validate performance in Tab. 9. This strongly influences the results on the validation data. This can be critical for sensitive applications where negative predictions can have more impact than positive (or vice-versa), such as cancer classification, where false negatives can endanger patients and erode human-machine trust.

5 Conclusion

We highlight that scalar activations deemed Super Neurons can serve as strong and robust categorical classifiers while improving runtime efficiency of VLMs. SNs compare favorably with the base models they are extracted from and sparse attention vectors, while enabling discovery of a large amount of accurate scalars in shallower layers of the LLM. This enables *extreme early exiting* during the generation of the *first token* and in the *first layer* of the LLM, substantially reducing inference time. We plan to apply our method for vision language action models, in which accurate discrete action decisions could be taken faster.

Limitations. Future research should be conducted to determine whether Super Neurons are able to provide useful signals on complex open-ended prompts and reasoning and if robustness and early exiting still hold in these contexts.

Table 9: Impact of metric optimization for SNs discovery. We use LLaVA-v1.5-7b on INSTORDER (OCC.). Willingly optimizing for a given metric μ results in significant performance improvements in the subsequent measure.

Metric	Method	Metric optimization (μ)	
		Accuracy	F1
Accuracy	SNs (mean)	64.5	25.6
	SNs (maj. voting)	78.2	67.0
Precision	SNs (mean)	23.5	16.4
	SNs (maj. voting)	30.4	24.6
Recall	SNs (mean)	61.8	98.4
	SNs (maj. voting)	36.5	59.7
F1	SNs (mean)	34.0	28.1
	SNs (maj. voting)	33.2	34.9

Acknowledgements

We would like to thank Ryan Teehan, Vivian Lee and Kyunghyun Cho for the helpful discussions and advice on improving this manuscript. We thank NYU for providing some of the GPU resources to support this work.

References

- Bai, S., Cai, Y., Chen, R., Chen, K., Chen, X., Cheng, Z., Deng, L., Ding, W., Gao, C., Ge, C., Ge, W., Guo, Z., Huang, Q., Huang, J., Huang, F., Hui, B., Jiang, S., Li, Z., Li, M., Li, M., Li, K., Lin, Z., Lin, J., Liu, X., Liu, J., Liu, C., Liu, Y., Liu, D., Liu, S., Lu, D., Luo, R., Lv, C., Men, R., Meng, L., Ren, X., Ren, X., Song, S., Sun, Y., Tang, J., Tu, J., Wan, J., Wang, P., Wang, P., Wang, Q., Wang, Y., Xie, T., Xu, Y., Xu, H., Xu, J., Yang, Z., Yang, M., Yang, J., Yang, A., Yu, B., Zhang, F., Zhang, H., Zhang, X., Zheng, B., Zhong, H., Zhou, J., Zhou, F., Zhou, J., Zhu, Y., Zhu, K.: Qwen3-VL Technical Report. CoRR **abs/2511.21631** (2025). <https://doi.org/10.48550/ARXIV.2511.21631>, <https://doi.org/10.48550/arXiv.2511.21631> 1, 9
- Bajpai, D.J., Hanawal, M.K.: FREE: Fast and Robust Vision Language Models with Early Exits (2025), <https://arxiv.org/abs/2506.06884> 3
- Black, K., Brown, N., Driess, D., Esmail, A., Equi, M., Finn, C., Fusai, N., Groom, L., Hausman, K., Ichter, B., et al.: π : A vision-language-action flow model for general robot control. CoRR, abs/2410.24164, 2024. doi: 10.48550. arXiv preprint ARXIV.2410.24164 (2024) 4
- Brown, T.B., Mann, B., Ryder, N., Subbiah, M., Kaplan, J., Dhariwal, P., Neelakantan, A., Shyam, P., Sastry, G., Askell, A., Agarwal, S., Herbert-Voss, A., Krueger, G., Henighan, T., Child, R., Ramesh, A., Ziegler, D.M., Wu, J., Winter, C., Hesse, C., Chen, M., Sigler, E., Litwin, M., Gray, S., Chess, B., Clark, J., Berner, C., McCandlish, S., Radford, A., Sutskever, I., Amodei, D.: Language Models are Few-Shot Learners. In: NeurIPS (2020) 1
- Cao, Q., Paranjape, B., Hajishirzi, H.: PuMer: Pruning and merging tokens for efficient vision language models. In: Proceedings of the 61st Annual Meeting of the Association for Computational Linguistics (Volume 1: Long Papers). pp. 12890–12903. Association for Computational Linguistics, Toronto, Canada (Jul 2023), <https://aclanthology.org/2023.acl-long.721> 3
- Cheng, A., Yin, H., Fu, Y., Guo, Q., Yang, R., Kautz, J., Wang, X., Liu, S.: SpatialRGPT: Grounded Spatial Reasoning in Vision-Language Models. In: NeurIPS (2024) 1
- Darcet, T., Oquab, M., Mairal, J., Bojanowski, P.: Vision Transformers Need Registers. CoRR **abs/2309.16588** (2023) 4
- Dubey, A., Jauhri, A., Pandey, A., Kadian, A., Al-Dahle, A., Letman, A., Mathur, A., Schelten, A., Yang, A., Fan, A., et al.: The llama 3 herd of models. arXiv e-prints pp. arXiv-2407 (2024) 1
- Fu, X., Hu, Y., Li, B., Feng, Y., Wang, H., Lin, X., Roth, D., Smith, N.A., Ma, W., Krishna, R.: BLINK: Multimodal Large Language Models Can See but Not Perceive. In: ECCV (23). Lecture Notes in Computer Science, vol. 15081, pp. 148–166. Springer (2024) 3

10. Gurari, D., Li, Q., Stangl, A.J., Guo, A., Lin, C., Grauman, K., Luo, J., Bigham, J.P.: Vizwiz grand challenge: Answering visual questions from blind people. In: Proceedings of the IEEE conference on computer vision and pattern recognition. pp. 3608–3617 (2018) [7, 1](#)
11. Hojel, A., Bai, Y., Darrell, T., Globerson, A., Bar, A.: Finding Visual Task Vectors. In: ECCV (43). Lecture Notes in Computer Science, vol. 15101, pp. 257–273. Springer, Springer (2024) [3](#)
12. Hu, E.J., Shen, Y., Wallis, P., Allen-Zhu, Z., Li, Y., Wang, S., Wang, L., Chen, W., et al.: Lora: Low-rank adaptation of large language models. ICLR **1**(2), [3](#) (2022) [3](#)
13. Huben, R., Cunningham, H., Smith, L.R., Ewart, A., Sharkey, L.: Sparse Autoencoders Find Highly Interpretable Features in Language Models. In: ICLR. OpenReview.net (2024) [4](#)
14. Jeddi, A., Baghbanzadeh, N., Dolatabadi, E., Taati, B.: Similarity-Aware Token Pruning: Your VLM but Faster (2025), <https://arxiv.org/abs/2503.11549> [3](#)
15. Johnson, J., Hariharan, B., Van Der Maaten, L., Fei-Fei, L., Lawrence Zitnick, C., Girshick, R.: Clevr: A diagnostic dataset for compositional language and elementary visual reasoning. In: Proceedings of the IEEE conference on computer vision and pattern recognition. pp. 2901–2910 (2017) [8, 1](#)
16. Kang, S., Kim, J., Kim, J., Hwang, S.J.: See What You Are Told: Visual Attention Sink in Large Multimodal Models. In: The Thirteenth International Conference on Learning Representations (2025), <https://openreview.net/forum?id=7uDI7w5RQA> [4](#)
17. Kang, S., Kim, J., Kim, J., Hwang, S.J.: Your Large Vision-Language Model Only Needs A Few Attention Heads For Visual Grounding. In: CVPR. pp. 9339–9350. Computer Vision Foundation / IEEE (2025) [1, 4](#)
18. Kim, M.J., Pertsch, K., Karamcheti, S., Xiao, T., Balakrishna, A., Nair, S., Rafailov, R., Foster, E., Lam, G., Sanketi, P., et al.: Openvla: An open-source vision-language-action model. arXiv preprint arXiv:2406.09246 (2024) [4](#)
19. Le, Q.V., Ranzato, M., Monga, R., Devin, M., Corrado, G., Chen, K., Dean, J., Ng, A.Y.: Building high-level features using large scale unsupervised learning. In: Proceedings of the 29th International Conference on Machine Learning, ICML 2012, Edinburgh, Scotland, UK, June 26 - July 1, 2012 (2012), <http://icml.cc/2012/papers/73.pdf> [3](#)
20. Lee, H., Park, J.: Instance-wise Occlusion and Depth Orders in Natural Scenes. In: CVPR. pp. 21178–21189. IEEE (2022) [7, 1](#)
21. Li, Y., Du, Y., Zhou, K., Wang, J., Zhao, W.X., Wen, J.R.: Evaluating Object Hallucination in Large Vision-Language Models. In: Proceedings of the 2023 Conference on Empirical Methods in Natural Language Processing. pp. 292–305 (2023) [7, 1, 2](#)
22. Liang, Y., Wang, Z., Xu, X., Zhou, J., Lu, J.: Efficientllava: Generalizable auto-pruning for large vision-language models. In: Proceedings of the Computer Vision and Pattern Recognition Conference. pp. 9445–9454 (2025) [3](#)
23. Liu, H., Li, C., Wu, Q., Lee, Y.J.: Visual Instruction Tuning. In: NeurIPS (2023) [1, 9, 3](#)
24. Liu, Y., Wang, Y., Shi, B., Zhang, X., Dai, W., Li, C., Xiong, H., Tian, Q.: Meteor: Multi-encoder collaborative token pruning for efficient vision language models. In: Proceedings of the IEEE/CVF International Conference on Computer Vision. pp. 21492–21504 (2025) [3](#)

25. Liu, Z., Zhu, L., Shi, B., Zhang, Z., Lou, Y., Yang, S., Xi, H., Cao, S., Gu, Y., Li, D., et al.: Nvlla: Efficient frontier visual language models. In: Proceedings of the Computer Vision and Pattern Recognition Conference. pp. 4122–4134 (2025) [1](#), [3](#), [9](#)
26. Lu, P., Mishra, S., Xia, T., Qiu, L., Chang, K., Zhu, S., Tafjord, O., Clark, P., Kalyan, A.: Learn to Explain: Multimodal Reasoning via Thought Chains for Science Question Answering. In: Advances in Neural Information Processing Systems 35: Annual Conference on Neural Information Processing Systems 2022, NeurIPS 2022, New Orleans, LA, USA, November 28 - December 9, 2022 (2022), http://papers.nips.cc/paper_files/paper/2022/hash/11332b6b6cfc4485b84afadb1352d3a9a-Abstract-Conference.html [8](#), [2](#)
27. Mitra, C., Huang, B., Chai, T., Lin, Z., Arbelles, A., Feris, R., Karlinsky, L., Darrell, T., Ramanan, D., Herzig, R.: Enhancing Few-Shot Vision-Language Classification with Large Multimodal Model Features. In: Proceedings of the IEEE/CVF International Conference on Computer Vision (ICCV). pp. 2760–2772 (October 2025) [1](#), [2](#), [3](#), [4](#), [5](#), [9](#), [12](#), [14](#)
28. Musacchio, P., Lee, H., Park, J.: Holistic Order Prediction in Natural Scenes. In: The Thirty-ninth Annual Conference on Neural Information Processing Systems (2025), <https://openreview.net/forum?id=RVkuARTXet> [7](#), [1](#), [2](#)
29. Oikarinen, T., Weng, T.W.: Clip-dissect: Automatic description of neuron representations in deep vision networks. ICLR (2022) [4](#)
30. OpenAI: ChatGPT (2023), <https://chat.openai.com>, large language model developed by OpenAI, based on the GPT-4 architecture [1](#)
31. Oquab, M., Darcet, T., Moutakanni, T., Vo, H.V., Szafraniec, M., Khalidov, V., Fernandez, P., Haziza, D., Massa, F., El-Nouby, A., Assran, M., Ballas, N., Galuba, W., Howes, R., Huang, P., Li, S., Misra, I., Rabbat, M., Sharma, V., Synnaeve, G., Xu, H., Jégou, H., Mairal, J., Labatut, P., Joulin, A., Bojanowski, P.: DINOv2: Learning Robust Visual Features without Supervision. Trans. Mach. Learn. Res. **2024** (2024) [4](#)
32. Radford, A., Józefowicz, R., Sutskever, I.: Learning to Generate Reviews and Discovering Sentiment. CoRR [abs/1704.01444](https://arxiv.org/abs/1704.01444) (2017), <http://arxiv.org/abs/1704.01444> [3](#)
33. Radford, A., Kim, J.W., Hallacy, C., Ramesh, A., Goh, G., Agarwal, S., Sastry, G., Askell, A., Mishkin, P., Clark, J., Krueger, G., Sutskever, I.: Learning Transferable Visual Models From Natural Language Supervision. In: ICML. Proceedings of Machine Learning Research, vol. 139, pp. 8748–8763. PMLR (2021) [1](#)
34. Schwenk, D., Khandelwal, A., Clark, C., Marino, K., Mottaghi, R.: A-OKVQA: A Benchmark for Visual Question Answering Using World Knowledge. In: Computer Vision - ECCV 2022 - 17th European Conference, Tel Aviv, Israel, October 23-27, 2022, Proceedings, Part VIII. pp. 146–162 (2022). https://doi.org/10.1007/978-3-031-20074-8_9, https://doi.org/10.1007/978-3-031-20074-8_9 [8](#), [1](#), [2](#)
35. Skean, O., Arefin, M.R., Zhao, D., Patel, N., Naghiyev, J., LeCun, Y., Shwartz-Ziv, R.: Layer by Layer: Uncovering Hidden Representations in Language Models. CoRR [abs/2502.02013](https://arxiv.org/abs/2502.02013) (2025) [1](#), [4](#)
36. Tang, S., Wang, Y., Kong, Z., Zhang, T., Li, Y., Ding, C., Wang, Y., Liang, Y., Xu, D.: You need multiple exiting: Dynamic early exiting for accelerating unified vision language model. In: Proceedings of the IEEE/CVF conference on computer vision and pattern recognition. pp. 10781–10791 (2023) [3](#)
37. Tang, Z., Lian, L., Eisape, S., Wang, X., Herzig, R., Yala, A., Suhr, A., Darrell, T., Chan, D.M.: TULIP: Towards Unified Language-Image Pretraining. CoRR [abs/2503.15485](https://arxiv.org/abs/2503.15485) (2025) [3](#)

38. Templeton, A., Conerly, T., Marcus, J., Lindsey, J., Bricken, T., Chen, B., Pearce, A., Citro, C., Ameisen, E., Jones, A., Cunningham, H., Turner, N.L., McDougall, C., MacDiarmid, M., Freeman, C.D., Sumers, T.R., Rees, E., Batson, J., Jermyn, A., Carter, S., Olah, C., Henighan, T.: Scaling monosemanticity: Extracting interpretable features from claude 3 sonnet. Transformer Circuits Thread (2024), <https://transformer-circuits.pub/2024/scaling-monosemanticity/index.html> 4
39. Touvron, H., Martin, L., Stone, K., Albert, P., Almahairi, A., Babaei, Y., Bashlykov, N., Batra, S., Bhargava, P., Bhosale, S., Bikel, D., Blecher, L., Canton-Ferrer, C., Chen, M., Cucurull, G., Esiobu, D., Fernandes, J., Fu, J., Fu, W., Fuller, B., Gao, C., Goswami, V., Goyal, N., Hartshorn, A., Hosseini, S., Hou, R., Inan, H., Kardas, M., Kerkez, V., Khabsa, M., Kloumann, I., Korenev, A., Koura, P.S., Lachaux, M., Lavril, T., Lee, J., Liskovich, D., Lu, Y., Mao, Y., Martinet, X., Mihaylov, T., Mishra, P., Molybog, I., Nie, Y., Poulton, A., Reizenstein, J., Rungta, R., Saladi, K., Schelten, A., Silva, R., Smith, E.M., Subramanian, R., Tan, X.E., Tang, B., Taylor, R., Williams, A., Kuan, J.X., Xu, P., Yan, Z., Zarov, I., Zhang, Y., Fan, A., Kambadur, M., Narang, S., Rodriguez, A., Stojnic, R., Edunov, S., Scialom, T.: Llama 2: Open Foundation and Fine-Tuned Chat Models. CoRR **abs/2307.09288** (2023) 1
40. Wang, T., Zhou, W., Zeng, Y., Zhang, X.: EfficientVLM: Fast and Accurate Vision-Language Models via Knowledge Distillation and Modal-adaptive Pruning. In: ACL (Findings). pp. 13899–13913. Association for Computational Linguistics (2023) 3
41. Ye, X., Gan, Y., Ge, Y., Zhang, X.P., Tang, Y.: Atp-llava: Adaptive token pruning for large vision language models. In: Proceedings of the Computer Vision and Pattern Recognition Conference. pp. 24972–24982 (2025) 3
42. Yu, Z., Lee, Y.J.: How Multimodal LLMs Solve Image Tasks: A Lens on Visual Grounding, Task Reasoning, and Answer Decoding. CoRR **abs/2508.20279** (2025) 1, 4, 12
43. Zhang, Q., Cheng, A., Lu, M., Zhuo, Z., Wang, M., Cao, J., Guo, S., She, Q., Zhang, S.: [CLS] Attention is All You Need for Training-Free Visual Token Pruning: Make VLM Inference Faster. arXiv preprint arXiv:2412.01818v1 (2024) 3
44. Zitkovich, B., Yu, T., Xu, S., Xu, P., Xiao, T., Xia, F., Wu, J., Wohlhart, P., Welker, S., Wahid, A., et al.: Rt-2: Vision-language-action models transfer web knowledge to robotic control. In: Conference on Robot Learning. pp. 2165–2183. PMLR (2023) 4

Taking Shortcuts for Categorical VQA Using Super Neurons

Supplementary Materials

Pierre Musacchio¹, Jaeyi Jeong², Dahun Kim³, and Jaesik Park¹

¹ Seoul National University

² EPFL

³ Google Deepmind

{pmusacchio, jaesik.park}@snu.ac.kr

A Datasets and prompts

We describe the dataset along with the prompts used for probing and validation in more detail in this section.

POPE. POPE is a dataset designed to evaluate the degree of hallucinations of VLMs. Built on top of COCO, it consists of 2.9K VQA that relate to the presence or absence of objects in images. Broadly speaking, to visual hallucinations [21].

INSTAORDER (OCC.). INSTAORDER also stems from COCO and consists of instance-wise ordering annotations. Recent work converted this dataset into a B-VQA format and observed that LLaVA-v1.5-7b struggles to answer such geometry-related prompts. This split of the dataset tests the models’ understanding of instance-wise occlusions [20, 28].

INSTAORDER (DEPTH). Second split of INSTAORDER, the questions contained in this challenge test the models’ abilities to reason about instance-wise depth order.

VIZWIZ. Created by people with visual impairments, VIZWIZ is a general benchmark aiming at testing models’ capacities to reason under constrained visual inputs. We filter the dataset on “yes”-“no” answers and only keep such questions for both the probing and validation sets [10].

CLEVR. To test our method’s generalization capabilities on synthetic data, we select CLEVR. This dataset evaluates the spatial understanding of the model through questions that span from counting to positional understanding. We filter this dataset to only retain classification questions for probing and validation [15].

A-OKVQA. A-OKVQA is an MCQ dataset of with four answer choices consisting of general visual world knowledge. Questions require commonsense reasoning grounded in the scene in order to be accurately answered [34].

Table 1: Prompt templates. We detail the templates used for some of the VQA datasets. {} indicates variables, obj indicates the object category, loc indicates the location of the object in a bounding box format and. For MCQ data, q indicates the original question and a_i indicates the i -th MCQ answer.

Dataset	Ref.	Prompt
POPE	[21]	Is there a {obj} in the image?
INSTAORDER (OCC.)	[28]	Is the {obj} at position {loc} obstructing the {obj} at position {loc}? Answer the question using a single word.
INSTAORDER (DEPTH.)	[28]	Is the {obj} in front of the {obj} at position {loc} from the viewer’s perspective? Answer the question using a single word.
A-OKVQA	[34]	{q} Is it { a_i }? Answer with yes or no.
SCIENCEQA	[26]	{q} Is it { a_i }? Answer with yes or no.

Table 2: Default configurations of the LLaVA-v1.5-7b and Qwen3-VL-4b-Instruct we use for all the experiments throughout our work.

(a) LLaVA-v1.5-7b configuration.

dtype	float16
model_type	llava
head_dim	128
hidden_act	silu
hidden_size	4096
model_type	llama
num_attention_heads	32
num_hidden_layers	32
num_key_value_heads	32
vocab_size	32064

(b) Qwen3-VL-4b-Instruct configuration.

dtype	float16
model_type	qwen3_vl
head_dim	128
hidden_act	silu
hidden_size	2560
model_type	qwen3_vl_text
num_attention_heads	32
num_hidden_layers	36
num_key_value_heads	8
vocab_size	151936

SCIENCEQA. We benchmark our approach on this high school science dataset. The SCIENCEQA dataset contains 26 topics, 127 categories, and 379 skills [26]. We convert this MCQ data to a series of binary visual question answer and perform inference in the same way as on the other datasets.

Prompts. For CLEVR and VIZWIZ, we do not apply any prompt template and simply filter the dataset to retain only “yes”-“no” VQA in both the training and validation sets. We prompt the model with the filtered samples. For the other datasets, we report the prompt templates we use in Tab. 1.

Note that for INSTAORDER, the location of the object is only specified if there are multiple same object categories in the image. This allows disambiguation of the target object. Otherwise, only the object category is specified.

Table 3: SNs compared to finetuned LLaVA alternatives on INSTAORDER. Given an annotation budget N , we compare both training time and task performances. We use the pretrained model of [23] as our baseline and their official finetuning script without altering any of the hyperparameters. For our approach, we report the results from the method obtaining the best F1 based on Tab. 2. Best results are in **bold**. Baseline is highlighted in **gray**, while our super neurons are in **yellow**.

Method	N	Training time	Data generalization	Occlusion performances				Depth performances			
				Acc.	Precision	Recall	F1	Acc.	Precision	Recall	F1
<i>LLaVA-v1.5-7b</i>	753k	8 h. [23]	X	64.9	18.5	40.2	25.3	65.0	66.4	80.2	72.6
<i>LLaVA-v1.5-7b-sft</i>	3k	2m.	X	14.8	14.8	100.0	25.8	57.9	57.9	100.0	73.4
<i>LLaVA-v1.5-7b-sft</i>	10k	5m.	X	82.1	43.5	71.2	54.0	75.1	83.1	71.5	76.9
<i>LLaVA-v1.5-7b-sft</i>	100k	49m.	X	83.7	47.1	81.8	59.8	79.8	83.8	80.8	82.3
<i>LLaVA-v1.5-7b-LoRA</i>	3k	2m.	X	67.5	23.9	54.7	33.3	55.4	58.8	76.4	66.5
<i>LLaVA-v1.5-7b-LoRA</i>	10k	5m.	X	83.0	45.2	69.8	54.8	75.1	84.8	69.5	76.4
<i>LLaVA-v1.5-7b-LoRA</i>	100k	41m.	X	84.4	48.5	81.2	60.7	80.2	84.1	81.3	82.7
Super Neurons	3k	0m.	✓	64.5	23.5	61.8	34.0	65.2	66.4	80.9	72.9

B Baselines

Baseline configurations. We report the configurations of LLaVA-v1.5-7b and Qwen3-VL-4b-Instruct used in our experiments in Tab. 2a and Tab. 2b. We do not alter these configurations unless specified otherwise in the paper.

Finetuned baselines comparison. We compare Super Neurons to fully finetuned and LoRA-tuned [12] LLaVA [23] at different dataset scales in Tab. 3. We use a dataset on which LLaVA is known to struggle to clearly identify the data scale at which finetuning begins to outperform SNs. For a small annotated finetuning budget, SNs obtain better results than finetuned alternatives while being training-free. On the other hand, as the annotation budget grows, fully finetuning the model becomes a better alternative if the goal is to improve performance for a *single task*. In fact, finetuning the model on a single task can lead to significant degradation on other tasks. In contrast, our training-free approach maintains the model’s general capabilities by preserving the pretrained weights.

C Profiling

We run an in-depth profiling benchmark using finer-grained measurements on an NVIDIA A100 GPU while varying the maximum generated token of the model (Tab. 4). We use LLaVA-v1.5-7b from the huggingface library. SNs, by skipping the autoregressive process of the network, dramatically decreases the wall time to obtain an answer. Most of the gain comes from bypassing (i) the autoregressive nature of the transformer, and (ii) avoiding the huggingface’s post-processing routine. Our approach is still $1.8\times$ faster than the base model when capping the model’s maximum number of generated tokens at 1.

Table 5: Prompt robustness. We use LLaVA-v1.5-7b on INSTAORDER (OCC.). We replace the comparative word in the prompt template with alternative words and evaluate compare the base model performances to the SNs performances.

Comparative word		<u>obstructing</u>		<u>hiding</u>		<u>occluding</u>		Random	
Split	Metric	Base	SNs	Base	SNs	Base	SNs	Base	SNs
Probe	Acc.	53.9	62.7	45.6	62.6	48.8	64.2	49.5	60.0
	F1	46.1	69.0	61.6	67.9	64.3	67.6	65.0	67.0
Validation	Acc.	64.9	78.2	16.2	68.1	18.3	66.8	17.9	66.9
	Prec.	18.5	30.4	13.9	24.2	14.6	23.8	14.7	22.2
	Recall	40.2	36.5	89.8	54.1	92.8	56.5	94.3	49.2
	F1	25.3	33.2	24.1	33.5	25.2	33.5	25.4	30.6

D Robustness

Prompt sensitivity. After investigating the robustness to dataset transfer in Sec. 4.4, we investigate the sensitivity of SNs to prompts. On the INSTAORDER (OCC.) dataset, the prompt template involves a relational word between the two compared instances (cf. Tab. 1). We replace that relational word with alternatives and report the results in Tab. 5. We find that SNs are robust to the choice of initial prompt, as shown by their similar F1 scores.

To push this idea, we also create a dataset that consists of random comparative strings formed by sampling 3-10 characters at random. Interestingly, SNs perform better than the vanilla model on this set as well suggesting that SNs encode general in-domain knowledge for a given task. This is due to the fact that we are directly extracting SNs from a metric that evaluates the task of interest.

Adversarial prompting. On the other hand, these numbers might hint that SNs could be overfitting or exploiting spurious bias from input data to produce their answers. To verify this, we lead two experiments using LLaVA-v1.5-7b on POPE. We choose POPE since performance on this dataset is already saturated and revolves around questions related to class recognition that can be subject to dataset class imbalance, allowing us to better perceive potential overfitting. We create two adversarial datasets:

- POPE-Im: we shuffle all the images of the validation set of POPE,
- POPE-Txt: we shuffle all the prompts of the validation set of POPE.

We evaluate SNs on these datasets in Tab. 6. Results show that when the prompt is not grounded in the image (and vice versa), SNs fail to answer accurately, and

Table 4: Profiling LLaVA-v1.5-7b on an NVIDIA A100 GPU using the huggingface’s inference routine (in s.). Ours is benchmarked on the first layer of the LLM.

Model	Max new toks.	Embedding	Prefix	Decoding	Wall time
LLaVA-v1.5-7b 128		0.032	0.085	0.025	1.01
LLaVA-v1.5-7b 1		0.032	0.086	0.024	0.223
SNs	1	0.032	0.085	0.002	0.119 _(-1.9x)

Table 6: Adversarial prompting. We evaluate LLaVA-v1.5-7b on adversarial POPE-Im and POPE-Txt validation datasets containing shuffled VQA pairs. SNs results on the original dataset is highlighted in gray.

Metric	Method	Dataset		
		POPE-Im	POPE-Txt	POPE
Accuracy	SNs (mean)	60.4	60.4	90.9
	SNs (maj. voting)	60.3	61.6	90.9
Precision	SNs (mean)	71.2	71.4	92.6
	SNs (maj. voting)	68.2	69.9	91.0
Recall	SNs (mean)	38.9	38.9	89.5
	SNs (maj. voting)	43.2	44.9	91.4
F1	SNs (mean)	50.3	50.3	91.0
	SNs (maj. voting)	52.9	54.6	91.2

the F1 score collapses. This indicates that while the prompt must have a degree of relevance to the image, SNs are likely not leveraging spurious biases or overfitting to either the prompt or the image to come up with their decisions. This claim is emphasized by the fact that SNs can generalize to novel distributions as shown in Tab. 7 of the main paper.

E Location of SNs

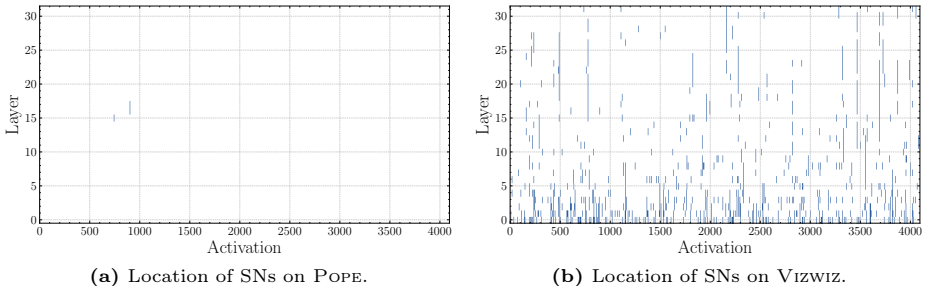


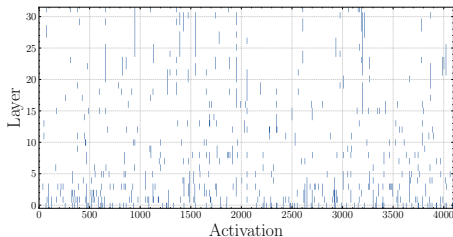
Fig. 1: Visualization of SNs on different datasets. We use LLaVA-v1.5-7b. We only visualize SNs that obtain better performances than the model itself. Few SNs emerge on the datasets that are already very well answered by the model, while we observe a significant amount of SNs on harder datasets.

Dataset-wise. We visualize the location of SNs for different datasets in Fig. 1. We use LLaVA-v1.5-7b and only report SNs that perform better than the network itself. In Fig. 1a, we observe that a few SNs perform better than the model. We hypothesize that this is because the model already answers POPE correctly. Yet, results in Tab. 2 show that these SNs are still useful for improving the model’s performance while dramatically reducing runtime Tab. 5.

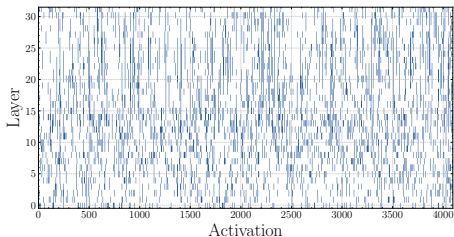
On the other hand, we observe that datasets for which LLaVA-v1.5-7b struggles naturally result in the emergence of many more SNs (Fig. 1b). Interestingly, a lot of them appear to be located in the shallower layers of the model.

Cross-dataset. To observe if some neurons share multiple types of expertise, we plot a heatmap of overlapping SNs on different datasets in Fig. 2. We only consider the neurons that exceed the model’s performance on *all* of the indicated datasets. We observe that some neurons indeed capture useful information across multiple tasks, suggesting they are part of an underlying decision process within the network. Moreover, this allows us to hypothesize potential links between different types of questions. Such a heatmap offers a new lens for understanding task relations and task proximity. In the future, we plan to explore the correlation between task proximity and SNs overlap.

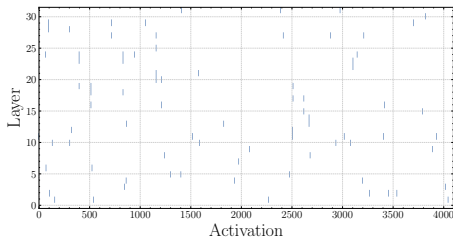
Of particular interest, we note that INSTAORDER (OCC.) and CLEVR share the largest number of SNs. This can be explained by the similarity between the questions in the two datasets that both target object-wise geometric understanding (Fig. 2b), but also because the base LLaVA-v1.5-7b does not perform well on these benchmarks. We find cases of SNs that surpass the model’s performance on three datasets at the same time (Fig. 2e) and a surprising case where a single neuron obtains better performances than LLaVA-v1.5-7b on all four benchmarks in Fig. 2f. This indicates that sparse activations in the form of Super Neurons constitute a lightweight and powerful representation that can generalize across diverse types of data.



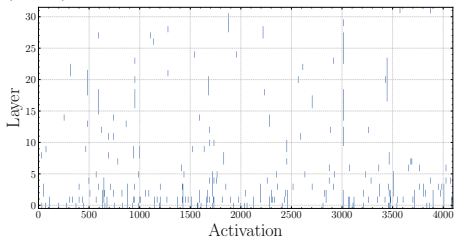
(a) Overlapping SNs between VIZWIZ and CLEVR.



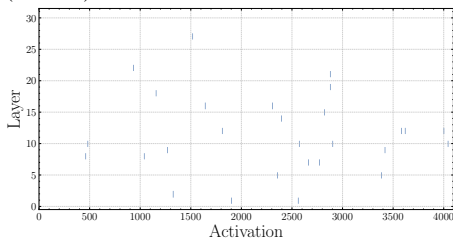
(b) Overlapping SNs between INSTAORDER (Occ.) and CLEVR.



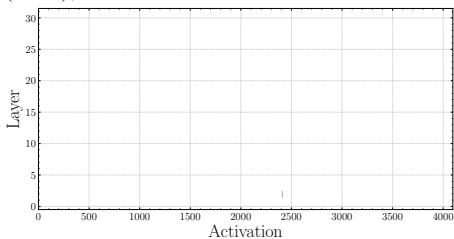
(c) Overlapping SNs between INSTAORDER (DEPTH.) and CLEVR.



(d) Overlapping SNs between INSTAORDER (Occ.), VIZWIZ and CLEVR.



(e) Overlapping SNs between INSTAORDER (Occ.), INSTAORDER (DEPTH.) AND CLEVR.



(f) Overlapping SNs between INSTAORDER (Occ.), INSTAORDER (DEPTH.), VIZWIZ and CLEVR.

Fig. 2: SNs overlap between different datasets. We visualize the probed neurons that surpass the model’s performance on all the indicated datasets. We use LLaVA-v1.5-7b. x -axis indicate neuron index while y -axis indicates layer index. Depending on the dataset pair, many SNs can overlap. We also find a quadruplet of datasets sharing SNs.